JOURNAL OF CATALYSIS 133, 247–259 (1992)

Ru/SiO_2-Impregnated and Sol-Gel-Prepared Catalysts: Synthesis, Characterization, and Catalytic Properties

T. LOPEZ, P. BOSCH, M. ASOMOZA, AND R. GOMEZ

Universidad Autonoma Metropolitana—Iztapalapa, Department of Chemistry, P.O. Box 55-534, Mexico D.F. 09340 Mexico

Received July 9, 1990; revised June 7, 1991

Impregnation and sol-gel preparation methods are compared. Only when prepared by sol-gel synthesis, ruthenium is incorporated in the silica network; RuO_2 particles are observed, but most Ru is occluded in the silica network. The ruthenium migrates to the surface with thermal treatments and small particles are formed. In the case of impregnated catalysts only RuO_2 particles are observed. Their diameter is larger when the catalyst is treated at high temperatures. *ortho*-Xylene hydrogenation was performed on these two kinds of catalysts. The deactivation and selectivity values are attributed to the structural differences of the catalysts.

INTRODUCTION

The discovery of metal support interaction has initiated new and vigorous studies on metal supported catalysts (*1–3*). The nature of this interaction has been attributed to an electronic effect (metal-support electron transfer) (*4–6*), or to contamination of metal particles by the support (*7–11*).

Platinum (*4, 5, 7*), palladium (*6, 12*), or rhodium (*13, 14*) has generally been chosen to study metal support effects. Indeed, they are very active metals and are not easily deactivated. Nevertheless ruthenium is known to be more active than platinum or palladium for many reactions of hydrocarbons (*15–17*), although it is difficult to study supported Ru because of its high rate of deactivation (*18*). In the case of supported ruthenium, preparation methods determine the structure of the final solids (*19–22*). It seemed, therefore, interesting to study metal-support effects in Ru/SiO_2. The catalysts of this work were prepared by impregnation and also by a nonconventional technique, sol-gel, whose advantages are as follows:

(1) The support is synthesized from an organometallic compound (alkoxide) containing dissolved ruthenium from the beginning of the reaction. Hence, the resulting products have a very high purity. The main advantage of the sol-gel preparation is the solution homogeneity (alkoxide + solvent + H_2O + Ru salt), which gels after a precise reaction time. The reactions describing the phenomenon are shown in Fig. 1.

(2) An inorganic network including Ru is easily formed. Silanol ($\equiv$Si—OH) and ethoxy ($\equiv$Si—OEt) intermediates condense. Nucleophiles ($\equiv$Si—O^-) then interact with the partially dissociated $RuCl_3$ and $\equiv$Si—O—Ru species are generated. The resulting gel contains a considerable amount of water and ethanol. These are desorbed at 110°C and organic groups disappear at 350°C, but the silica surface remains partially hydroxylated even at high temperatures (*23*). Metal oxide particles (RuO_2) have been detected by X-ray diffraction and the size and shape of the corresponding peaks are different from the size and shape observed in impregnated catalysts (*24*).

(3) When these catalysts were tested with benzene hydrogenation and *n*-pentane hydrogenolysis reactions, a metal-support effect was observed. It was explained as a

0021-9517/92 $3.00

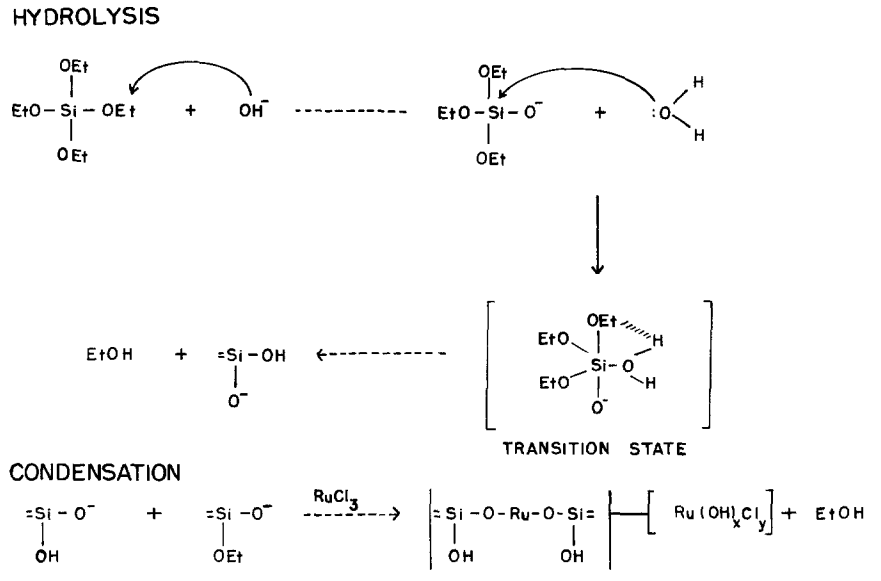

FIG. 1. Gelation of catalyst precursors.

metal-support interaction via surface OH groups (*25*). Still, ruthenium is easily deactivated by coke formation: partially dehydrogenated aromatic hydrocarbons polymerize and give rise to coke. In Ru/SiO_2 (sol-gel), deactivation is greatly diminished because polymerization deactivation reactions are structure sensitive, and in these catalysts small SiO_2 islands on the metallic particle surface are present (*25*).

One would expect that the possible role of metal-support effects would be magnified in catalysts prepared by the sol-gel method, giving the promising results of previous work (*9, 24, 25*). The objectives of the present work are to describe the metal-support interaction between Ru and SiO_2, and to explain mechanistically structural changes in the catalysts. The *o*-xylene hydrogenation reaction is used as a catalytic test for structural features and support interactions.

EXPERIMENTAL

Catalyst Preparation

Ru–SG–3. Tetraethoxysilane, 24.1 ml, was refluxed with 10 ml of ethanol, 1.5 ml of NH_4OH, and 0.444 g of $RuCl_3 \cdot 3\ H_2O$ for 10 min. Afterward 10 ml of water was added and the reflux was maintained until gel formation. The metal content was 3 wt% Ru.

Ru–Imp–3. Six grams of sol-gel silica (i.e., silica prepared from tetraethoxysilane at pH 9 and calcined at 400°C in air for 12 h) was conventionally impregnated with a solution obtained by adding 20 ml of water to 0.462 g of $RuCl_3 \cdot 3\ H_2O$. The metal content was again 3 wt% Ru. The resulting catalysts were dried at 70°C for 12 h in air (fresh catalysts) and then calcined at 200, 400, 600, and 800°C for 4 h in air.

Characterization Techniques

IR and UV–VIS (diffuse reflectance). The catalysts, as solids, were characterized by IR spectroscopy with a MX-1 Fourier Transform Nicolet spectrometer. Pressure was applied to the catalyst powder (no KBr was used) until the pellet was transparent. The UV–VIS (diffuse reflectance) spectra were obtained with a Cary 17D Varian spectrograph.

X-ray diffraction techniques. A Siemens D 500 diffractometer coupled to a copper anticathode X-ray tube was used to obtain

the diffraction pattern of each catalyst. The Cu$K\alpha$ wavelength was provided by a nickel filter. When RuO_2 peaks were observed, they were measured by step scanning.

X-ray diffractograms were also obtained with a molybdenum anticathode X-ray tube. The Mo$K\alpha$ radiation was used with a diffracted beam monochromator, making it possible to reach the recommended high values of the angular parameter ($s = (4\pi \sin\theta)/\lambda$, where θ is the diffraction angle and λ the wavelength). The intensity values, read at intervals $\Delta\ 2\theta = (\frac{1}{8})°$ from $2\theta = 3°$ to $2\theta = 130°$ were the input data for the Magini and Cabrini program (*26*). The radial distribution function was then obtained and interpreted in terms of the reported interatomic distances.

The small angle X-ray diffraction curves were obtained with a Kratky camera. In this case, a Zr filter selected the Mo$K\alpha$ radiation. As the beam was "infinitely high," the particle size distributions were obtained in the "two-phase" case (*27*). The particle geometry was assumed to be spherical; this hypothesis, as shown elsewhere (*28*), is a good approximation. Instead of volume distributions, surface distributions are presented to facilitate the comparison with adsorption measurements (*29*). As a reference, a mean diameter was also estimated from the SAXS surface area values: $\bar{D} = 6/(\rho S)$; ρ is the density and S the surface area. This surface area is obtained from the Porod coefficient and has been discussed by Renouprez *et al.* (*28*).

Catalytic Experiments

The *o*-xylene hydrogenation was performed in a conventional differential flow reactor coupled to a gas chromatograph in order to analyze the products of the reaction. The reaction rate measurement was carried out at atmospheric pressure and 100°C. The partial pressures were 3.9 and 756 Torr for *o*-xylene and hydrogen, respectively. The products detected under these conditions were only 1,2-*cis*- and *trans*-dimethylcyclohexanes. The conversion of *o*-xylene was kept below 5.0% by varying the catalyst masses. During the reaction some deactivation was noted as a function of time.

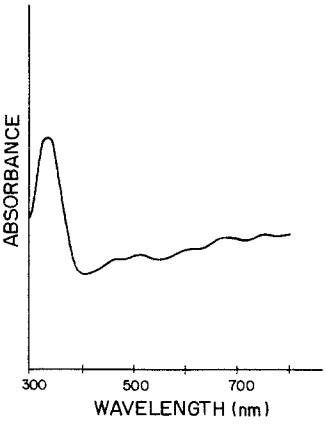

FIG. 2. Fresh Ru–SG–3 catalyst UV–VIS (diffuse reflectance) spectrum.

RESULTS

UV–VIS (diffuse reflectance) study. In our sol-gel catalysts, the ruthenium compound was a d^5 complex whose basal state configuration is $[2\,t_{1g}(xy, xz, yz)]^5$. This type of complex has an intense charge transfer absorption band in the ultraviolet. In the visible spectrum four bands due to *d-d* transitions were observed. These four bands have an intensity much lower than that of the charge transfer band. In Fig. 2 the fresh Ru–SG–3 catalyst spectrum is shown. The intense charge transfer band found at 325 nm must be assigned to an electron transfer between chlorine ions π orbitals and d metal orbitals [$\pi\ 1T_{2u} \rightarrow 2\ t_{2g}$]. The other *d-d* bands can be attributed to the following transitions between basal state and the excited states of the metal d orbitals (*30, 31*):

$$^2T_{2g} — {}^4T_{1g} \quad (750\text{ nm})$$

$$^2T_{2g} — {}^4T_{2g} \quad (600\text{ nm})$$

$$^2T_{2g} — {}^2A_{2g} \quad (680\text{ nm})$$

$$^2T_{2g} — {}^2A_{1g} \quad (500\text{ nm}).$$

Two of these transitions are spin-forbidden and are often observed as shoulders, whereas the allowed transitions have a high intensity band.

Nucleophiles ≡Si—O$^-$ interact with the metal atoms and weaken the Ru—Cl bond. Also, Ru can be coordinated to the H_2O molecules present in the reacting environment as well as with support OH groups producing the hexacoordinated complex $[RuCl_x(OH)_y(H_2O)_z]$ on the support surface.

The fresh Ru–Imp–3 catalyst has a spectrum very similar to that of the fresh Ru–SG–3; the only significant difference is the fading of the band observed at 600 nm and a small shift of CT and *d-d* bands. Such a fading can be attributed to the absence of H_2O in Ru–Imp–3 in the metal coordination sphere. The *d-d* bands are slightly shifted toward low energy because in Ru–Imp–3 catalyst, nucleophiles ≡Si—O$^-$ do not interact with the metal.

IR spectroscopy study. The characteristic IR bands of the catalysts are shown in Fig. 3. The fresh Ru–SG–3 spectrum has a band at 3837 cm^{-1} and a shoulder at 3420 cm^{-1} attributed to OH groups. Water and ethanol incorporated into the gel structure are the cause of the four small peaks in the 3600 to 3450 cm^{-1} region, but the main peak (3400 cm^{-1}) is due to silanol groups. At 2929, 2898, and 2352 cm^{-1} come three sharp peaks corresponding to C—H stretching vibrations (symmetric and asymmetric) of ethoxy groups occluded in the gel. The water O—H bending band is at 1628 cm^{-1}. In the low-energy zone of the spectrum, silica bands are observed, 1176 and 1082 cm^{-1} (Si—O stretching vibration), 801 and 614 cm^{-1} (Si—O$^-$ bending vibration), and 466 cm^{-1} ($^-$O—Si—O$^-$ bending vibration). This catalyst also has a band at 1394 cm^{-1}, which is characteristic of the H—C—H bending vibration of an ethoxy group. At 965 cm^{-1} one finds the stretching Si—OH vibration that masks the Ru—O vibration.

If the catalyst is calcined at 200°C, the bands at 3800 and 3400 cm^{-1} disappear and only a single weak band remains; the same

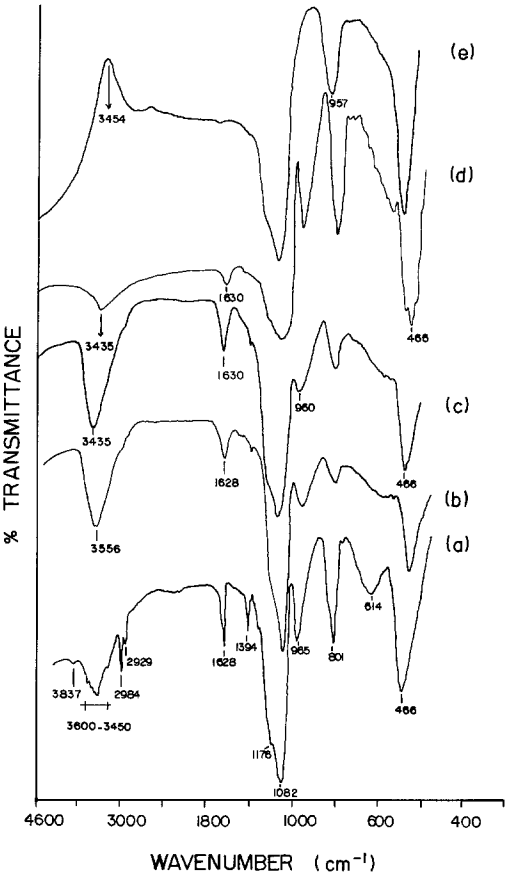

FIG. 3. IR spectra of Ru–SG–3 catalysts: (a) fresh, (b) 200°C treated, (c) 400°C treated, (d) 600°C treated, and (e) 800°C treated.

happens with the 1628 cm^{-1} band, which decreases in size until fading. These modifications are caused by loss of occluded water as well as by dehydration:

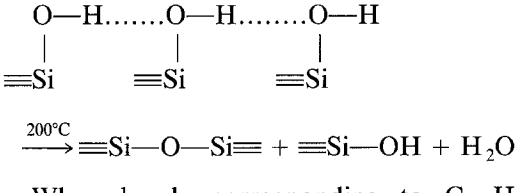

When bands corresponding to C—H bonds disappear, organic groups are not present in the sample. The silica bands shift to slightly lower frequencies.

If the solid is treated at 400 and 600°C the Si—OH stretching band moves to 3435

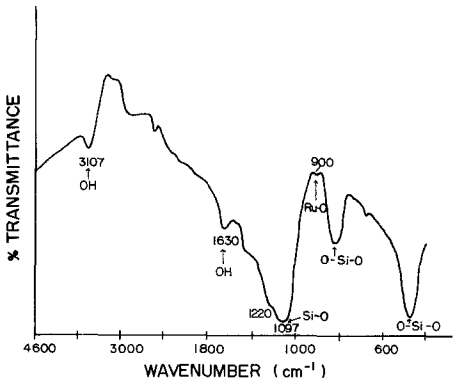

FIG. 4. IR spectrum of Ru–Imp–3 catalyst (400°C treated).

cm^{-1} as the structure is modified. Hydroxyl groups are now weakly bonded to the surface. At 800°C only a band at 3197 cm^{-1} is observed indicating that silica is partially hydroxylated even at that temperature. The silanol's band at 960 cm^{-1} fades entirely, at 600°C and, in that frequency range, only the 957 cm^{-1} band due to the Ru—O bond remains.

In the case of the conventionally impregnated catalyst (Ru–Imp–3) treated at 400°C in air, the IR spectrum is similar to the sol-gel preparation but with remarkable shifts. The OH stretching band is found at 3107 cm^{-1} because, as there is no metal incorporated in the silica network, the strength of the Si—OH bond diminishes. An OH bending vibration and an Si—OH stretching vibration are located at 1630 and 949 cm^{-1}, respectively. In this preparation the sol-gel silica is chemically stable before impregnation. Typical bands of the support are shifted to higher frequencies (i.e., Si—O stretching: 1220, 1097 and Si—O bending: 662, 473 cm^{-1}). The Ru—O band is now located at 900 cm^{-1}, which is the expected value for Ru—O bond in RuO_2; see Fig. 4.

X-ray diffraction. Conventional X-ray diffraction results have been summarized in a previous paper (*24*). In impregnated as well as sol-gel preparations (Ru–Imp–3 and Ru–SG–3), RuO_2 was identified but the size and the shape of the studied peaks (110 and 101) varied. If 400 and 800°C Ru–Imp–3 catalyst diffractograms are compared, RuO_2 peaks in 400°C treated solid are clearly asymmetric. In the case of the Ru–SG–3 catalysts such asymmetry is not observed but the RuO_2 peak, in the 400°C treated sol-gel solid, is very small.

Radial distribution function. As expected, each peak of silica sol-gel corresponds to an interatomic distance in amorphous silica; i.e., Si—O = 1.72 Å, Si—Si = 2.95 Å; Si—O = 4.16 Å; and Si—Si = 5.05 Å. The interpretation has been conducted in terms of the well-known studies reported by Warren *et al.* (*32*).

If it is assumed that the Ru–Imp–3 (400°C) is just a mixture of SiO_2 and RuO_2, its radial distribution function should be a series of peaks corresponding to the SiO_2 and RuO_2 interatomic distances (RuO_2: 2.07, 2.29, 3.11, 3.57, and 4.55 Å). In Fig. 5, the measured radial distribution function of the 400 and 800°C Ru–Imp–3 are compared.

Let us first discuss the 400°C treated cata-

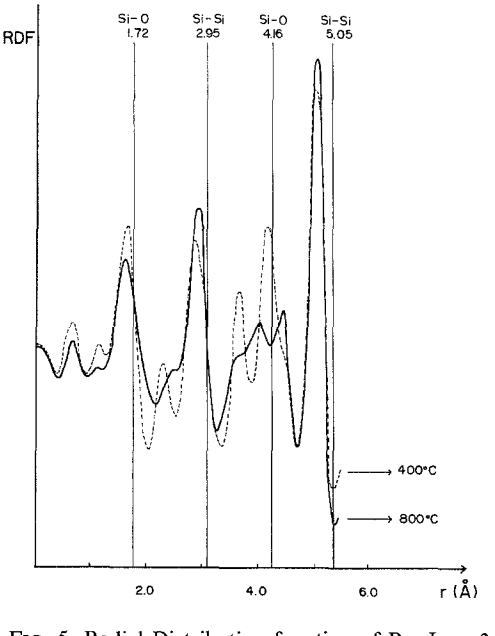

FIG. 5. Radial Distribution function of Ru–Imp–3: (— 800°C; ---- 400°C).

TABLE 1

Radial Location (Å) of the Peaks Present in Ru–Imp–3 Catalysts

SiO_2 (bibliography)		SiO_2 (this work)	Ru–Imp–3		RuO_2 (estimated)	
			400°C	800°C		
Si–O	r = 1.70	1.72	1.64	1.57	Ru–O	r = 2.07
			2.31	2.44		
					O–O	r = 2.29
Si–Si	r = 2.55	2.95	2.86	2.91		
					Ru–O	r = 3.11
		3.60 (shoulder)	3.67	3.63		
					Ru–Ru	r = 3.57
Si–O	r = 4.20	4.16	4.16	4.01		
			4.44 (shoulder)	4.44	Ru–Ru	r = 4.55
Si–Si		5.05	5.04	5.03		

lyst. The peaks corresponding to the silica are easily recognized (r = 1.64, 2.86, 4.16, and 5.03 Å), albeit slightly shifted from the pure silica values. Peaks of 2.31, 3.67, and 4.44 Å remain to be accounted for, thus they must be attributed to RuO_2 interatomic distances. Again, these values are shifted from those expected for a pure RuO_2 crystal. In Table 1, the peak to peak comparison is presented; note that only the first two SiO_2 peaks are slightly displaced; this shift falls into the experimental uncertainty ($\Delta r \cong \pm$ 0.05 Å). It is known that the larger the radial distances (r) the smaller the errors.

If the catalyst Ru–Imp–3 is treated at 800°C the radial distribution is slightly modified. First, the long-range order peaks are narrower and better resolved; for instance the peak at 4.44 Å is now very well defined. Hence, the material is more crystalline. But again, if this radial distribution function is compared to the radial distribution function of the 400°C treated material, the shifts in the peak positions do not seem to be significant as they fall in the range of experimental error.

Figure 6 and Table 2 summarize our results in the case of the sol-gel catalysts (Ru–SG–3). The 400°C treated catalyst is the most interesting and must be explained first. The Si—O distance (in SiO_2 tetrahedra) is again lower than the one found in pure silica. A peak at r = 2.10 Å is clearly resolved but the peak at r = 2.44 Å is not seen. It turns out that the sum of ionic radii (Ru^{+4} and O^{-2}) is exactly 2.07 Å: ruthenium is then bonded to oxygen but not as in the RuO_2 structure, it must be occluded into the silica network. Then comes the 2.93 Å peak which must be attributed to a Si—Si distance. The next peak, at r = 3.70 Å, can be due to a Ru—Ru distance in RuO_2.

If Ru–SG–3 is treated at 800°C, the silica

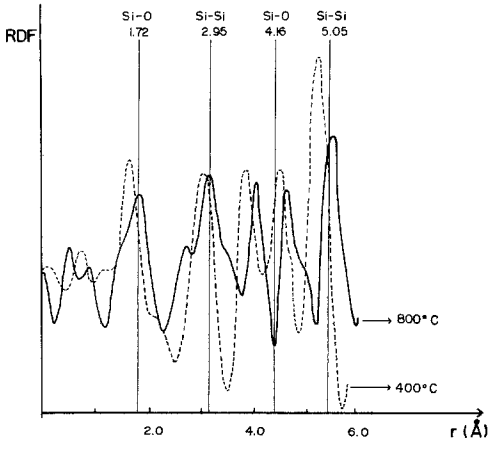

FIG. 6. Radial Distribution function of Ru–SG–3: (— 800°C; ---- 400°C).

TABLE 2

Radial Location (Å) of the Peaks Present in Ru–SG–3 Catalysts

	SiO_2 (this work)	Ru–SG–3		RuO_2 (estimated)	
		400°C	800°C		
Si–O	r = 1.72	1.59	1.79		
		2.10		Ru–O	r = 2.07
				(in silica network)	
			2.63	O–O	r = 2.29
Si–Si	r = 2.95	2.93	3.06		
	3.60	3.70	3.90	Ru–O	r = 3.11
	(shoulder)				
				Ru–Ru	r = 3.57
Si–O	r = 4.16	4.31	4.45		
Si–Si	r = 5.05	5.02	5.29		

network tends to assume a pure silica structure. The distance r = 2.10 Å assigned to a particular Ru environment disappears. It seems then that these Ru—O bonds perturb the silica network; instead, the distance r = 2.63 Å is now observed. This value must be correlated to the 2.44 Å value found in Ru–Imp–3 (800°C). The environment must be very similar to the one found in the Ru–Imp–3 sample, i.e., RuO_2 particles and noncrystalline SiO_2. This observation is confirmed if peaks at 3.90 and 4.45 Å are compared to 4.01 and 4.44 Å peaks found in the Ru–Imp–3 (800°C).

Small angle X-ray scattering. The particle size distribution of Ru–Imp–3 (400°C) has two maxima, the first one at D = 12 Å and the other one at D = 44 Å; Fig. 7. These values are in agreement with the mean diameter obtained from Porod's law. If the Ru–Imp–3 catalyst is treated at 800°C, the mean diameter is 66 Å and the particle size distribution maxima are located at 18 and 48 Å. As expected, the RuO_2 particles have sintered. Although such behavior can be predicted in impregnated catalysts, this is not the case in sol-gel catalysts.

The particle size distribution of the Ru–SG–3 (400°C) is broad (from D = 54 Å to D = 116 Å), the maximum of the distribution is found at D = 94 Å; Fig. 8. If the mean diameter is estimated from the SAXS specific surface value, it is $\bar{D}$ = 267 Å. Thus,

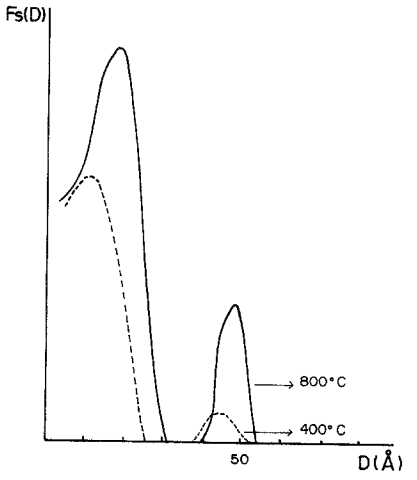

FIG. 7. Particle size distribution of Ru–Imp–3: (— 800°C; ---- 400°C).

a large portion of particles have a size larger than 150 Å and the particle size distribution shown here does not represent all the particles. If the Ru–SG–3 is treated at 800°C, the mean diameter is 120 Å. The particle size distribution maxima are now found at 42 and 72 Å. In this case, metal particles are smaller than those found in the Ru–SG–3 (400°C) preparation. Table 3 summarizes these results.

Catalytic activity. In Table 4, activities and selectivities for the various catalysts are

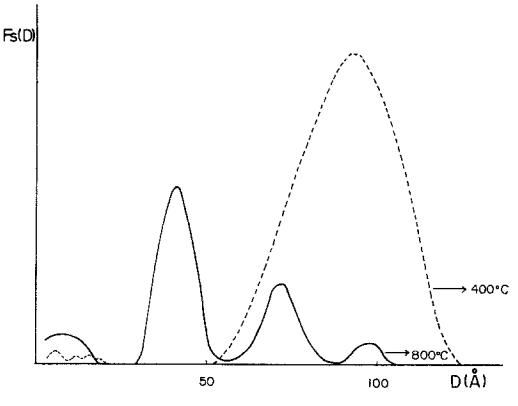

FIG. 8. Particle size distribution of Ru–SG–3: (— 800°C; ---- 400°C).

TABLE 3

SAXS Results, the Mean Diameter Obtained from Porod Approximation ($\bar{D}$) Is Compared to the Particle Size Distribution Maxima

Catalysts	Temperature	$\bar{D}$ (Å)	Particle size dist. maxima (Å)	
Ru–Imp–3	400°C	33	12	44
Ru–Imp–3	800°C	66	18	44
Ru–SG–3	400°C	267		94
Ru–SG–3	800°C	120	42	72

reported. Since deactivation occurs as a function of time, initial rates and the deactivation constant were calculated applying Levenspiel's model (*33*) in a manner similar to that used for Rh/Al_2O_3 catalysts (*34*).

The model is for parallel deactivation with a rate described by

$$\text{rate} = K_d C_A^n a,$$

where a, the fractional remaining activity decreases as

$$-\frac{da}{dt} = K_d C_a^{n'} a^d.$$

K_d is the rate constant for the deactivation reaction, C_A is the reactant A concentration, n is the reaction order for conversion of reactant A, n' is the order of concentration dependency of the deactivation, and d is the order of deactivation.

The Levenspiel approach is to hold C_A constant in time and space, lumping constants

$$K' = KC_A^n \quad \text{and} \quad K'_d = K_d C_a^{n'}.$$

The integrated result is

$$\left(\frac{WC_{A0}}{F_{A0}}\right)^{(d-1)} = \left(\frac{C_{A0} - C_A}{K'}\right)^{(d-1)} + \left(\frac{C_{A0} - C_A}{K'}\right)^{(d-1)} (d-1) K'_d t,$$

where F_{A0} is the feed rate and W is the mass of catalyst. This can be rearranged to give

$$\frac{1}{X^{(d-1)}} = \left(\frac{F_{A0}}{K'W}\right)^{(d-1)} + \left(\frac{F_{A0}}{K'W}\right)^{(d-1)} (d-1) K'_d t,$$

where X is the fractional conversion. Now if deactivation is second order, $d = 2$ (*34*) and if the conversion is so low (<5%) that the concentration can be considered constant throughout the reactor and throughout the duration of the experiment, the slope (K_e) is proportional to the lumped deactivation rate constant (K'_d) divided by the initial reaction rate (K'). The experimental slope obtained following the Levenspiel's model

TABLE 4

Activity, Selectivity, and Deactivation Constants for Ru/SiO_2 Catalysts in the *o*-xylene Hydrogenation at 100°C

Catalysts	K_e (10^3) (min^{-1})	K' (10^7) (mol/g cat s)	K'_d(10^{10}) ($K_e \cdot K'$)	S (%)	Activity $K'\bar{D}$ (a.u.)
Ru–Imp–3 (400°C)	3.2	21.3	68	95	703
Ru–Imp–3 (800°C)	153.8	4.4	670	96	290
Ru–SG–3 (400°C)	33.2	8.1	270	95	2162
Ru–SG–3 (800°C)	1.7	11.3	20	93	1356

Note. K_e, experimental slope; K', initial rate; K'_d, deactivation constant; S, selectivity (% of 1,2 *cis*-dimethylcyclohexane).

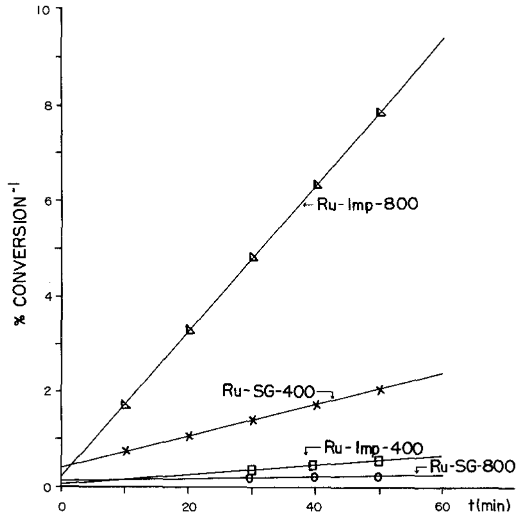

FIG. 9. Deactivation of *o*-xylene hydrogenation of Ru/SiO$_2$ catalysts treated in air at different temperatures: (X) Ru–SG–3 (400°C); (□) Ru–Imp–3 (400°C); (○) Ru–SG–3(800°C); (△) Ru–Imp–3 (800°C).

for the Ru–Imp–3 and Ru–SG–3 catalysts is shown in Fig. 9.

The experimental values of the slope K_e (obtained from the Levenspiel model), the initial reaction rate K', and the deactivation constant K_d' are reported in Table 4. The results show that the deactivation constant depends strongly on the temperature treatments and on the preparation method of the catalysts. The highest value of K_d' corresponds to the 800°C Ru–Imp–3 catalyst and the smallest value is obtained in 800°C Ru–SG–3 samples. Note, also, in this table that the initial rates as well as the selectivities to the *cis* product are less sensitive to such effects. It seems, then, that in sol-gel catalysts the principal effect of the preparation method (i.e., impregnation of the support or addition of the precursor into the gel) is observed on the side reactions such as deactivation.

DISCUSSION

Structure

The X-ray diffraction results must be interpreted in terms of bulk structure. The main difference between ruthenium impregnated and ruthenium sol-gel solids treated at 400°C is a peak at r = 2.10 Å in the radial distribution function. Also, an asymmetric large peak is seen in X-ray diffractograms, if the catalyst is impregnated, but only a small peak is observed if the catalyst is prepared via the sol-gel technique. Therefore Ru, in impregnated catalysts, is oxidized as RuO$_2$ and the structure of the solid can be visualized as noncrystalline SiO$_2$ support and small RuO$_2$ particles whose crystallinity is not perfect (strain between planes).

The Ru–SG–3 (400°C) has RuO$_2$ metal particles; the silica support is not crystalline but some ruthenium was detected to be in a nonrutile-like crystallographic system. As the preparation is homogeneous, it is difficult to accept that ruthenium, linked to oxygens (from the support) is inhomogeneously distributed. Therefore, ruthenium must be incorporated in the silica network.

Such a proposition is strengthened by FTIR measurements. In Ru–Imp–3 (400°C) catalyst, the IR bands are shifted to higher frequencies, but the band due to the Ru—O bond is found at 900 cm^{-1} (as in RuO$_2$). Then the following mechanism can be proposed:

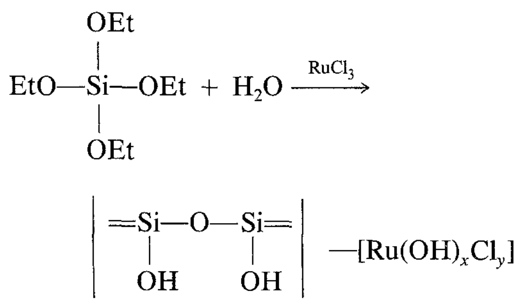

Ruthenium is octahedrally coordinated on the support surface as was shown by UV–VIS spectroscopy.

Instead, in the Ru–SG–3 (400°C) sample, the Ru—O IR band is found at 957 cm^{-1}, the shift to higher energy shows that Ru—O bond strength increases in the catalyst. Such shifts suggest that some ruthenium must be incorporated in the silica network (Fig. 1).

The structure shown in Fig. 10 can be proposed to explain how ruthenium is oc-

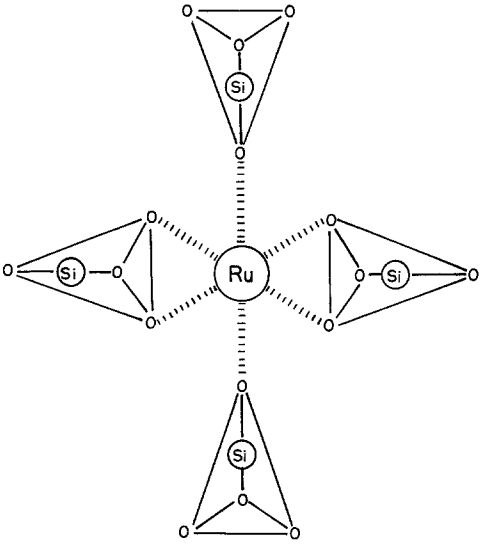

FIG. 10. Suggested structure of ruthenium atoms in the sol-gel silica network.

cluded into the silica network (*35*). Note that, although a chlorine–OH interaction is present in both preparations, it is stronger in sol-gel catalysts. Ruthenium is known to be easily coordinated to H_2O or OH groups; in sol-gel catalysts, this bonding is favored because the metal is in contact with such species even before the gelation point. Hence, in 400°C treated solids, the Ru–Imp–3 structure is the conventional one. An interesting observation is that the particle crystallinity suffers strain. In Ru–SG–3, some ruthenium is incorporated into the silica network whose structure is distorted.

A predictable sintering occurs in the Ru–Imp–3 solid when it is treated at 800°C. In contrast, it seems that temperature treatment diminishes particle size of Ru–SG–3 catalysts. Furthermore, as shown by X-ray diffraction, the particles are well crystallized and more numerous. To explain such spontaneous generation of small RuO_2 particles, the following mechanism is proposed: some Ru is occluded into the silica network, as shown in the previous section. As it is weakly bonded to silica tetrahedra it is able to migrate as temperature is increased, then it seggregates to the surface and, there, it agglomerates and crystallizes as RuO_2 particles. Such a proposition is backed by the corresponding radial distribution functions: the interatomic distance $r = 2.10$ Å, attributed to ruthenium in the silica network and found in 400°C treated material, is not found in 800°C treated catalyst.

Surface Model

To explain catalytic test results in terms of the catalyst structure, a surface model must be proposed for each preparation technique. In Ru–Imp–3, the support is stabilized at 450°C for 4 h before the impregnation, as explained in the experimental section. Therefore, the metal is entirely on the surface. In addition to the RuO_2 identified by X-ray diffraction, an octahedral complex with the surface OH^- and Cl^- ions that cannot dissociate is formed. In the case of Ru–SG–3 fresh catalyst, from the first step of the reaction the metal is in contact with the alkoxide; enough solvent was added, of course, to ensure the best interaction between the reacting species. During tetraethoxysilane hydrolysis a nucleation process of the intermediary groups (ethoxy and silanols) occurs around ruthenium. When the condensation step begins, precursors of the inorganic network are formed in which the metal is octahedrally coordinated.

The gel is formed after 60 s of reaction. Ru acts, indeed, as a hydrolysis catalyst. As the gelation is so fast, there is a large number of ≡Si—OEt groups: they are not easily substituted by ≡Si—OH in the silica tetrahedron. To summarize, ethanol and water are occluded in the fresh gel structure and also in alkoxide organic groups that have not polymerized. The surface is then entirely hydroxylated. If the gel is treated at 110°C, water and solvent are eliminated, and at 350°C the alkoxide organic groups are desorbed (*23*). Some of the OH groups, weakly bonded to the surface, are lost at 450°C, although some OH groups still remain at 800°C. The elimination of these species con-

tributes to pore formation and, therefore, to a higher specific area (*24*). With calcination the network contracts and microcrystalline structures are generated around the metal atoms. Ru is located in the middle of the edges of silica tetrahedra. On the surface of Ru–SG–3, RuO_2 particles, as those found in Ru–Imp–3 catalyst, are present.

Catalytic Activity Effects

The most important results of Table 4 are those concerning the pretreatment effect and the preparation method in the ability of the catalysts to resist self-deactivation. The strong tendency of Ru to deactivate in hydrogenation reactions can be correlated to the coke formation due to the polymerization of partially hydrogenated species (*18*). The formation of coke depends on the particle size (*36*), coke precursor formation as metallo-carbenes or metallo-carbynes being favored on dense planes (*37, 38*). Deactivation then, must be more important in large particles than in small ones. These hypotheses agree well with the results on impregnated type catalysts; the K'_d of the 800°C Ru–Imp–3 catalyst (particle size around 66 Å) is higher than the one observed for 400°C Ru–Imp–3 catalyst (particle size 33 Å). The surprising fact of Table 4 is that the Ru–SG–3 catalyst shows a small deactivation constant that does not correspond to the large particle size exhibited. In sol-gel preparations the active metal is added during the sol formation and, as is shown by the spectroscopic studies, a fraction of the metal is occluded in the SiO_2 structure.

To obtain a good correlation between the particle size determined by X-ray diffraction and the catalytic behavior of the sol-gel catalysts two hypothesis can be advanced: (1) the determined large particle size corresponds to Ru conglomerates occluded into the network and small particles, deposited on the surface, are responsible for the catalytic effects; (2) the particles are large and are on the surface, but an unusual support effect operates in this case. The first hypothesis can be ruled out, because SiO_2 has a very high area (*24*) and Ru is very mobile (the specific surface BET area for the Ru–Imp–3 and Ru–SG–3 catalysts treated at 400°C in air are 300 and 500 m^2/g respectively). The second hypothesis requires an explanation on the possibility that large particles will act like small ones. The singular behavior of sol-gel catalysts must have its origin in the nature of the support. Sol-gel silica preparations have been found to be very highly hydroxylated surface solids. The metal particles are surrounded by Si—OH species. During the pretreatments in air such species can react: SiO_2 may be the resulting compound, and it may be deposited on the surface of the reduced metallic particles. This effect is similar to a particular size diminution and, then, the corresponding deactivation may be smaller.

The particle size determined from X-ray study is used to evaluate the activity per site ($K'\bar{D}$) of the catalysts (Table 4). The high activity observed for Ru–SG–3 catalysts cannot be explained by dispersion effects. Aromatic hydrogenation is an insensitive particle size reaction, at least for particles larger than 30 Å. By contrast, coke formation is a sensitive particle size reaction and for large particles a large deactivation must occur. As mentioned above, the deposit of SiO_2 on Ru particles can reduce the size of Ru ensembles on which carbon polymerization occurs. This would inhibit deactivation of the reaction by carbon and lead to an enhanced catalytic activity. Similar effects have been observed on Rh (*11*) and Ru (*10*) magnesia-supported catalysts. Magnesia is a support that hydrolyzes very easily during the impregnation step and the $Mg(OH)_2$ species react to produce MgO deposited on the metallic particles.

Additional evidence for the mechanical nature of the support effect by deposition of SiO_2 on the metallic particles was furnished by the selectivity values. *Cis* addition was found to be a structure sensitive reaction on Pd, Rh, and Ru silica-supported catalysts (*39, 40*). Small particles are electron-deficient and *cis* addition is diminished in the

higher coordinative unsaturation of small metal particles. As we propose a support effect analogous to a particle size diminution, *cis* addition must be modified in Ru–SG–3 catalysts. The very constant value of selectivity demonstrates that the electron-deficient effect does not operate in this case. Therefore, the deposited support on the metallic particles in sol-gel catalysts inhibits the polymerization of the partially hydrogenated hydrocarbons and consequently inhibits a fast deactivation. The metallic particles do not suffer any electronic modification and the selectivity to *cis* addition remains constant.

CONCLUSIONS

The following general trends emerge:

(a) The thermal treatment and the catalyst preparation determine the changes in interatomic distances of the silica network.

(b) At 400°C the Ru is partially incorporated into the silica network in the Ru–SG–3 catalyst. At 800°C it migrates to the surface and the SiO_2 acquires its own structure and composition.

The most important effect in catalytic activity for sol-gel catalysts is observed in the side reactions, i.e., self-deactivation. The highly hydroxylated support, can be deposited on the metallic particles. Such an effect would be comparable to a diminution of the particle size, giving smaller self-deactivation rates.

ACKNOWLEDGMENTS

P.B. thanks the Instituto Mexicano del Petroleo for the use of X-ray diffraction facilities and V. H. Lara for the technical help. Financial support from SEP-PROIDES is recognized. We are indebted to the referees for their helpful work.

REFERENCES

1. Bond, G. C., *in* "Metal-Support and Metal-Additive Effects in Catalysis (B. Imelik, C. Naccache, G. Coudurier, H. Praliaud, P. Meriadeau, P. Gallezot, G. A. Martin, and J. C. Vedrine, Eds.), Studies on Surface Science and Catalysis, Vol. 11, p. 1. Elsevier, Amsterdam, 1982.
2. Schwab, G. M., *in* "Advances in Catalysis" (D. D. Eley, H. Pines, and P. B. Weisz, Eds.), Vol. 27, p. 1. Academic Press, New York, 1978.
3. Solymosi, F., *Catal. Rev.* **1,** 233 (1967).
4. Gallezot, P., *Catal. Rev.-Sci. Eng.* **20,** 121 (1979).
5. Dalla Betta, R. A., and Boudart, M., *In* "Proceedings, 5th International Congress on Catalysis, Palm Beach, 1972" (J. W. Hightower, Ed.). North-Holland, Amsterdam, 1973.
6. Figueras, F., Gomez, R., and Primet, M., *Adv. Chem. Ser.* **121,** 480 (1973).
7. Tauster, S. J., Fung, S. C., Baker, R. T. K., and Horsley, J. A., *Science* **211,** 1121 (1981).
8. Resasco, D., and Haller, G., *J. Chem. Soc. Chem. Commun.,* 1150 (1980).
9. Lopez, T., Lopez-Gaona, A., and Gomez, R., J. *Non Crystallogr. Solids* **110,** 170 (1989).
10. Viniegra, M., Gomez, R., and Gonzalez, R. D., *J. Catal.* **111,** 429 (1988).
11. Poels, E. K., Magnus, P. J., van Velzen, J., and Ponec, V., *in* "Proceedings, 8th International Congress on Catalysis, Berlin, 1984," Vol 2, p. 59. Dechema, Frankfurt-am-Main, 1984.
12. Del Angel, G., Coq, B., Figueras, F., Fuentes, S., and Gomez, R., *Nouv. J. Chim.* **7,** 173 (1983).
13. Fenoglio, R. J., Nuñez, G. M., and Resasco, D. E., *J. Catal.* **121,** 77 (1990).
14. Fuentes, S., Figueras, F., and Gomez, R., *J. Catal.* **68,** 419 (1981).
15. Kubicka, H., *J. Catal.* **12,** 223 (1968).
16. Dun, J. A., and Scholten, J. J. F., *Faraday Discuss.* **72,** 145 (1982).
17. Schoenmaker, M. C., Verwijs, J. W., Don, J. A., and Scholten, J. J. F., *Appl. Catal.* **29,** 73 (1981).
18. Viniegra, M., Arroyo, V., and Gomez, R., *Appl. Catal.* **44,** 1 (1988).
19. Mieth, J. A., and Schawarz, J. A., *J. Catal.* **118,** 218 (1989).
20. Villamil, P., Reyes, J., Rosas, N., and Gomez, R., *J. Mol. Catal.* **54,** 205 (1989).
21. Narita, T., Miura, H., Sugiyama, K., Matzuda, T., and Gonzalez, R. D., *J. Catal.* **103,** 492 (1987).
22. Narita, T., Miura, H., Ohira, H., Sugiyama, K., Matzuda, T., and Gonzalez, R. D., *Appl. Catal.* **32,** 85 (1987).
23. Lopez, T., Asomoza, M., Razo, L., and Gomez, R., *J. Non Crystallogr. Solids* **108,** 45 (1989).
24. Lopez, T., Bosch, P., and Gomez, R., *React. Kinet. Catal. Lett.* **41,** 217 (1990).
25. Lopez, T., Lopez-Gaona, A., and Gomez, R., *Langmuir* **6,** 1343 (1990).
26. Magini, M., and Cabrini, A., *J. Appl. Crystallogr.* **5,** 14 (1972).
27. Soulé, J. L., *J. Phys. Radium* **18,** 90 (1957).
28. Renouprez, A. J., Hoang Van, C., and Compagnon, P. A., *J. Catal.* **34,** 411 (1974).
29. Brusset, H., and Donati, J. R., *J. Appl. Crystallogr.* **2,** 55 (1969).
30. Harizon, Z., and Navon, G., *Inorg. Chem.* **19,** 2236 (1980).

31. Jorgensen, K., *Acta Chem. Scand.* **10,** 518 (1956).
32. Warren, B. E., Krutter, H., and Morningstar, D., *J. Am. Ceram. Soc.* **19,** 202 (1936).
33. Levenspiel, D., *J. Catal.* **25,** 265 (1972).
34. Fuentes, S., Figueras, F., and Gomez, R., *J. Catal.* **68,** 419 (1981).
35. Pope, E. J. A., and Mackenzie, J. D., *J. Non Crystallogr. Solids* **106,** 236 (1988).
36. Coq, B., Bittar, A., and Figueras, F., *in* "Structure and Reactivity of Surfaces" (C. Morterra, A. Zecchina, and G. Costa, Eds, p. 327. Elsevier, Amsterdam, 1989.
37. Van Broekmouen, E. H., and Ponec, V., *J. Mol. Catal.* **25,** 109 (1984).
38. Ponec, V., *in* "Advances in Catalysis" (D. D. Eley, H. Pines, and P. B. Weisz, Eds.), Vol. 32, p. 42. Academic Press, San Diego, 1982.
39. Viniegra, M., Ph. D. thesis, UAM, 1990.
40. Viniegra, M., Cordoba, G., and Gomez, R., *J. Mol. Catal.* **58,** 107 (1990).